JOURNAL OF THERMOPHYSICS AND HEAT TRANSFER
Vol. 12, No. 2, April–June 1998

Experimental Investigation of the Multiple Scattering of a Polarized Laser Beam

A. Ambirajan* and D. C. Look Jr.†
University of Missouri–Rolla, Rolla, Missouri 65401

In this paper the forward-scattered diffuse radiation produced by a circularly polarized laser beam impinging on a finite plane-parallel scattering medium is studied experimentally. The radial variation of the forward-scattered Stokes vector is analyzed. Values of the degree of circular and linear polarization of the scattered radiation computed using experimental data are compared with values obtained using a Monte Carlo code. Trends with respect to the size parameters of the scatterers and the optical thickness are also presented. It was observed that the diffuse radiation is strongly polarized, even at large optical radii. This is true for all the size parameters and optical depths of the medium studied.

Nomenclature

C_{sca} = scattering cross section
D = geometric diameter of scatterer
$e[\cdots]$ = estimator
H = geometric depth of sample
$\boldsymbol{I}$ = Stokes vector
I, Q, U, V = components of the Stokes vector
I_0 = incident intensity
$\boldsymbol{I}_0$ = Stokes vector for the delta function loading
K = identity matrix
L = optical thickness of slab
$\boldsymbol{L}$ = rotation matrix
M = Stokes matrix
m = complex refractive index
N = number density of scatterers
$\bar{N}$ = number density of scatterers in the 10% latex solution
n_m = refractive index of the liquid carrier medium
P = phase matrix
P_{beam} = laser beam power, mW
P_c = degree of circular polarization
P_l = degree of linear polarization
P_t = degree of polarization
$p_{11}, p_{21}, s_{21}, d_{21}$ = elements of the Mie scattering matrix
r = optical radius
V = volume of liquid carrier medium
v = volume of 10% latex solution
x, y, z = optical coordinates
Z = scattering matrix
α, β, γ = variables of integration for higher scatter orders
β_e = extinction coefficient of the scattering medium
γ_1, γ_2 = limits to μ for single-scattered radiation
Θ = included angle during scattering
θ = polar angle
κ = absorbtion coefficient of water
λ = wavelength of the laser radiation
σ = rotation angle
ϕ = azimuthal angle
χ = size parameter, $n_m \pi D/\lambda$
ω = single-scattered albedo

Subscripts
e = exiting quantity
i = incident quantity

Superscript
T = transpose

I. Introduction

THE multiple scattering of radiant energy within a material is an area of considerable interest. In medical diagnostics, the analysis of scattered laser radiation from tissue samples is increasingly being used as a diagnostic tool.[1–4] The use of lasers in surgery also requires an understanding of the way in which laser radiation is scattered and absorbed by tissue.[4] Lasers are also being used for remote sensing in lidar systems.[5] Multiple scattering of radiant energy has been used in process applications to determine particle concentrations.[6] An isssue that has not received much attention in the literature is the effect of multiple scattering on the polarization of the diffuse radiation produced by a narrow beam of radiant energy such as a laser.

When a narrow linearly polarized beam of radiation is incident on a scattering medium, the backscattered radiant intensity exhibits a highly anisotropic pattern[7–12] (the bow-tie). Look[8] observed that this bow-tie had a cosine variation. When viewed through a crossed polarizer, a four-lobed pattern was also observed. Dogariu and Asakura[11] showed that the bow-tie was a consequence of the polarizing effect of single scattering, and was thus mainly observable for lower orders of scatter and small-size parameters. Dogariu and Asakura[12] also used the diffusion approximation to evaluate the cross-polarized component of backscattered radiation from a plane-parallel medium and obtained good results. These analyses thus indicate that polarization effects are propagated to significant distances in a scattering medium.

Mueller and Crosbie[13] present a formulation for three-dimensional radiative transfer with polarization using the integral transform method. They also developed certain spatial symmetry relationships for the reflection and transmission matrices. In a subsequent paper, Mueller and Crosbie[14] used this integral transform method and the symmetry relationships to obtain the functional form, i.e., of the bow-tie, of the spatially

Received Nov. 22, 1996; revision received Aug. 13, 1997; accepted for publication Sept. 29, 1997.

*Graduate Student, Thermal Radiative Transfer Group, Mechanical and Aerospace Engineering and Engineering Mechanics Department.

†Professor, Thermal Radiative Transfer Group, Mechanical and Aerospace Engineering and Engineering Mechanics Department. Associate Fellow AIAA.

varying reflection and transmission matrices for the multiple scattering of a polarized laser beam from a plane-parallel scattering medium composed of scatterers with a plane of symmetry. Their method is valid for any incident state of polarization and any axisymmetric spatial loading. Their transform technique, though exact, is time consuming to implement.

The backward Monte Carlo method has been used in studying the propagation of polarized radiation in scattering atmospheres.[15–18] Ambirajan and Look[18] suggested an algorithm to deal with the multiple scattering of a polarized narrow beam of radiation. In their paper, they present numerical results for the backscattered radiation produced by a circularly polarized narrow beam incident on a plane-parallel scattering medium for a number of size parameters of the scatterers and optical thicknesses of the medium. Ambirajan and Look's results[18] indicate that the radiation remains polarized to significant optical radii from the beam. Further, it was observed that the diffuse radiant energy was polarized despite having on average undergone a large number of scattering events. Their analysis, however, neglects the effect of Fresnel reflection at the boundary between the scattering and surrounding medium.

In the literature, there is not much experimental data characterizing the spatial variation of the diffuse radiation produced by a polarized laser beam. An early experimental study on the effects of the incident polarization state on the radial variation of the intensity backscattered by a plane-parallel scattering layer was conducted by Look.[19,20] Significant differences were observed in the backscattered intensity when a linearly polarized laser beam was incident on the medium as compared to the radial variation in the intensity when a circularly polarized laser beam impinged on the medium. Dogariu and Asakura[12] obtained a good fit between experimental data and calculations based on a modified diffusion approximation for the cross-polarized component of the diffuse radiation. However, they do not address the degree of polarization of the diffuse radiation. There have been a number of studies on the depolarization of polarized radiation by random media. Bicout and Brosseau,[21] in fact, conclude that after about 10 scattering events, a polarized beam of light is depolarized. Experimental data on the time-resolved depolarization of polarized incident radiation are supplied in Refs. 22–24. However, they do not tackle the spatial variation of the diffuse radiation field. Thus, the problem to be tackled in this paper is an experimental investigation of the diffuse radiation produced by a circularly polarized laser beam normally incident on a plane-parallel medium composed of scattering particles. The diffuse radiation produced by a circularly polarized laser beam is cylindrically symmetric about the laser beam[19,20]; thus, the variation in the intensity will depend only on the radial distance from the laser beam. In this paper, the forward-scattered Stokes vector of the diffuse radiation is measured with a view to understand radial variations in the degree of polarization of the diffuse radiation. Experimental data are compared to calculated values based on a backward Monte Carlo method developed by the authors.[18]

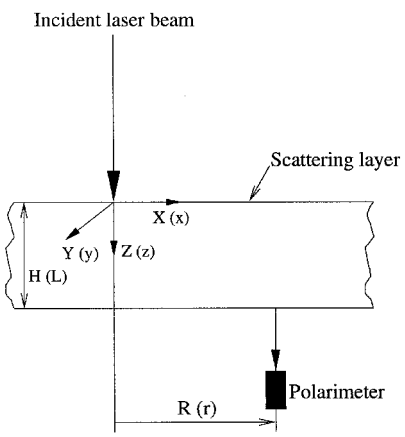

Fig. 1 Scattering geometry. The variables outside the parentheses are geometric and have the units of centimeters while those in the parenthesis are the corresponding optical coordinates. Note that the laser is normally incident on the medium.

II. Theory

In this paper the interaction of a polarized laser beam (see Fig. 1) with a plane-parallel scattering medium will be examined. In this section, some basic theory required to understand the multiple scattering process will be presented. First, the description of polarized radiation in terms of Stokes vectors will be outlined. Subsequently, the interaction of polarized radiation with the scattering medium will be characterized in terms of a matrix.

A. Radiation Field Description

In the theory of polarized radiative transfer, the state of polarization and intensity of a beam is specified by $\boldsymbol{I}$ in the following form:

$$\boldsymbol{I} = \begin{Bmatrix} I \\ Q \\ U \\ V \end{Bmatrix} \tag{1}$$

The elements Q, U, and V define the state of polarization of the light beam, and I denotes the intensity.[25]

Another quantity of interest in polarized radiative transfer is P_t. This is defined as

$$P_t = \sqrt{Q^2 + U^2 + V^2}/I \tag{2}$$

and indicates the fraction of the radiation that is polarized regardless of whether it is linear or circular. Similarly, P_l is defined by

$$P_l = \sqrt{Q^2 + U^2}/I \tag{3}$$

The quantity $\sqrt{Q^2 + U^2}$ represents the magnitude of linear polarization in the radiation. It, however, does not specify the orientation of the electric vector. Further, P_c is defined by

$$P_c = V/I \tag{4}$$

Also note that

$$P_t = \sqrt{P_l + P_c} \tag{5}$$

Throughout this paper, reference will be made to the depolarization of the diffuse light field. This implies a decrease in the degree of polarization.

B. Scattering Medium Description

In polarized radiative transfer theory, the scattering properties of a medium are defined by a quantity called the scattering matrix. The scattering matrix is a 4×4 matrix that transforms the Stokes vector of an incident beam of radiation to the Stokes vector of a scattered beam. The scattering matrix can be obtained experimentally,[26,27] or derived in a rigorous manner.[27,28] For scattering by a medium composed of spherical scatterers, the scattering matrix can be derived rigorously using Maxwell's equations with appropriate boundary conditions.[27,28] The form of this matrix is given by

$$Z(\Theta) = \begin{bmatrix} p_{11}(\Theta) & p_{21}(\Theta) & 0 & 0 \\ p_{21}(\Theta) & p_{11}(\Theta) & 0 & 0 \\ 0 & 0 & s_{21}(\Theta) & -d_{21}(\Theta) \\ 0 & 0 & d_{21}(\Theta) & s_{21}(\Theta) \end{bmatrix} \tag{6}$$

where $Z(\Theta)$ is a function of Θ between the incident and scattered beams of radiation, as shown in Fig. 2. All of the elements of the scattering matrix $Z(\Theta)$ are real. This scattering matrix operates on the incident Stokes vector [the **l** axis is assumed to be parallel to the scattering plane as shown in Fig. 2]. Note that in Fig. 2 the shaded region is the scattering plane. Each of the four independent functions [$p_{11}(\Theta)$, $p_{21}(\Theta)$, $s_{21}(\Theta)$, and $d_{21}(\Theta)$] in Eq. (6) is a function of the size parameter ($\chi = n_m \pi D/\lambda$) and the relative complex index of refraction ($m = n - i\kappa$) of the spherical scatterer. Each of these four functions and the coefficients of this series have been obtained rigorously.[29] A number of standard computer codes are available for the purpose of computing the coefficents of the Legendre series expansions of the preceding elements.[30,31] It should be noted that $p_{11}(\Theta)$ is normalized as follows:

$$\frac{1}{4\pi}\int_{4\pi} p_{11}(\Theta)\, d\Omega = 1 \tag{7}$$

where Ω is the solid angle. Note that p_{11} is the scalar Mie phase function.[28] In the case of Mie scattering, examples of the four elements of the scattering matrix are illustrated in Fig. 3 for a variety of size parameters.

In multiple-scattering problems, the **l** axes of the Stokes vectors, both incident and scattered, are assumed to be parallel to the meridional planes (planes of constant ϕ as seen in Fig. 2. The meridional planes for azimuthal angles of ϕ_1 and ϕ_2 are shown in Fig. 2. It can be seen in this figure that the **l** axes for both the incident and scattered beams are parallel to the meridional planes corresponding to ϕ_1 and ϕ_2, respectively. To compute the scattered Stokes vector at a particular location, the coordinate frame of the incident light beam must be rotated by an angle $\pi - \sigma_1$ (see Fig. 2) such that the **l** axis is parallel to the scattering plane. The scattering matrix then operates on this rotated Stokes vector. A subsequent rotation by $-\sigma_2$ brings the **l** axis parallel to the meridional plane of the scattered beam. The preceding rotations are mathematically equivalent to pre- and postmultiplying the scattering matrix by rotation matrices. Various papers outline this operation[13,25]; hence, only the final result will be given here. If the rotation operator is denoted by $L(\sigma)$, for a rotation of σ, then the phase matrix is given by

$$P(\mu_2, \phi_2; \mu_1, \phi_1) = L(-\sigma_2)Z(\Theta)L(\pi - \sigma_1) \tag{8}$$

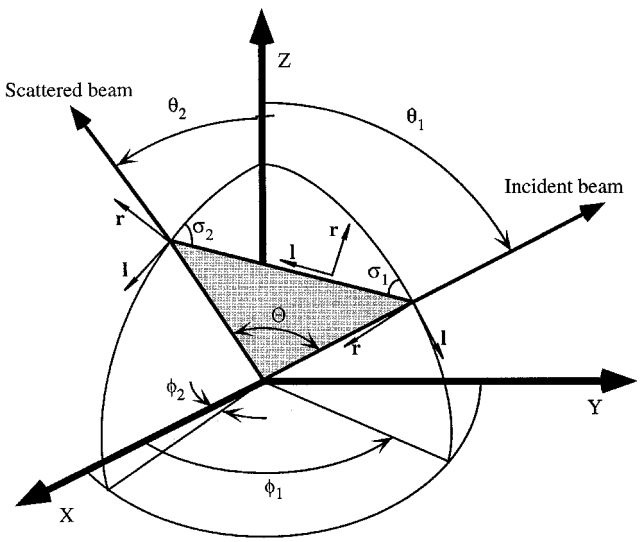

Fig. 2 Geometry of the rotation angles necessary in the phase matrix. Note that the shaded plane is the scattering plane. Light beams propagate in the r 3 l direction.

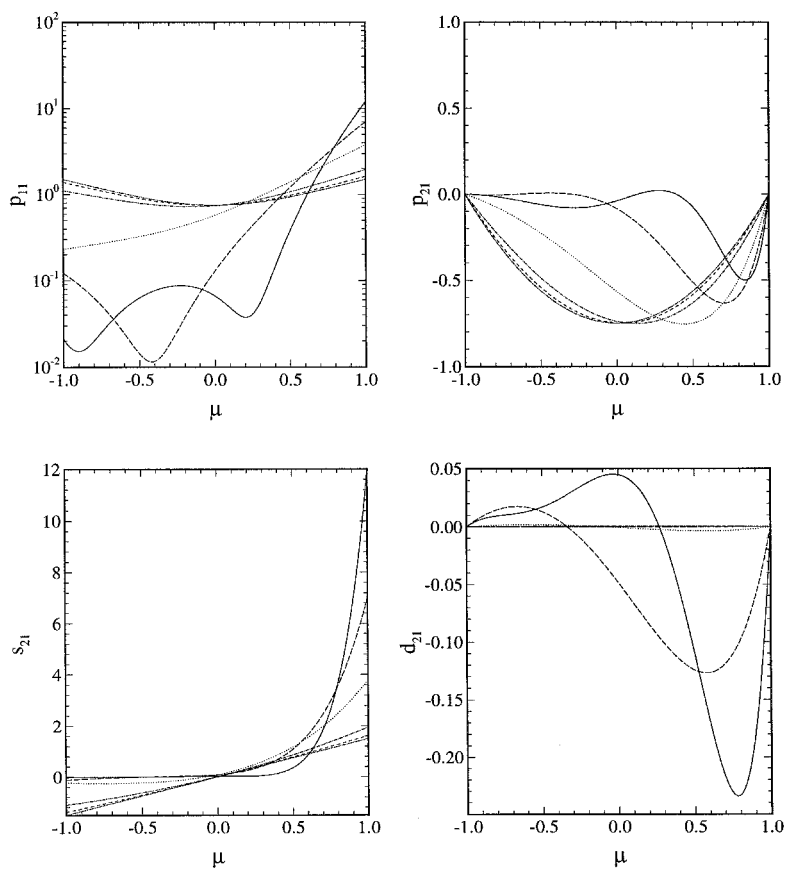

Fig. 3 Elements of the Mie phase matrix for m = 1.197 1 0*i* (-···-···-, Rayleigh; ---, x = 0.430; -·-·-, x = 0.813; ·····, x = 1.592; – – –, x = 2.379; ——, x = 3.264).

In the preceding equation, note that μ is the cosine of θ. σ can be found using spherical trigonometry. The relevant formulas for σ, Θ, and $L(\sigma)$ are given in an earlier paper by the authors.[18,25]

C. Optical Coordinate System

An important quantity in computing the optical coordinate in a scattering medium is the coefficient β_e, given by

$$\beta_e = NC_{sca} + \kappa \tag{9}$$

where κ is assumed negligible in this study. N is the number of scatterers per unit volume, and C_{sca} is the scattering cross section of the particles.[28] In this study, the scattering cross sections were computed using Mie theory[28] for a refractive index of $m = 1.197 + 0.000i$. This is the the relative refractive index for latex in water.[32] Note that for all computations in this paper, ω is taken to be unity.

If a volume of solution v with a known $\bar{N}$ and known C_{sca} is mixed with a volume V of water, then the resultant extinction coefficent of the medium is given by

$$\beta_e = v/(v + V)\bar{N}C_{sca} + \kappa \tag{10}$$

In this paper, either geometric coordinates (which have units of centimeters), or optical coordinates (which are nondimensional), will be specified. The optical coordinate in the X direction is defined to be x, i.e., $x = \beta_e X$. The same convention will apply for the Y and Z directions. The rectangular optical coordinate system chosen for this problem is shown in Fig. 1, with its origin at the point where the laser beam intersects the scattering medium.

III. Experimental Setup

In this section, various aspects of the experimental setup will be discussed. First, the overall goal of the present experiment will be presented. Subsequently, the actual experimental setup will be described. After this, the technique for the measurement of the Stokes vector will be briefly discussed.

A. Description of Experimental Setup

The goal in designing the experimental setup was to study the forward-scattered polarized diffuse radiation when a polarized laser beam was incident on a plane-parallel scattering medium. Our interest was primarily in the radial variation of certain polarization parameters of the diffuse radiation. This is illustrated in Fig. 1, where a laser beam is shown incident on a plane-parallel scattering medium. In this study, the scattering medium consists of latex particles suspended in pure distilled water. Note that L is the optical thickness of the scattering medium. A polarimeter (described in the next section) was used to measure the Stokes vector of this forward-scattered radiation.

A schematic of the experimental setup is presented in Fig. 4. The source of radiation was a 20-mW He–Ne (632.8-nm) laser with a beam diameter at the point of incidence with the scattering medium of 1.691 mm. The laser beam was passed through a prism, a linear polarizer, and a quarter wave plate (QWP). These components were used to control the state of polarization of the incident beam on the scattering medium. The sample cell containing the scattering medium is cylindrical and coated on the inside with flat black paint. The bottom of the sample cell is a glass window. The i.d. of the sample cell is 9.80 cm. The volume of the cell is 250 cc, which corresponds to a height H of the scattering medium of 3.31 cm. Cemented to the glass window is a small light trap where the unscattered portion of the incident laser is absorbed. The polarimeter below the sample cell was on an Aerotech X–Y translation stage with a positional accuracy of 10 μm. The position

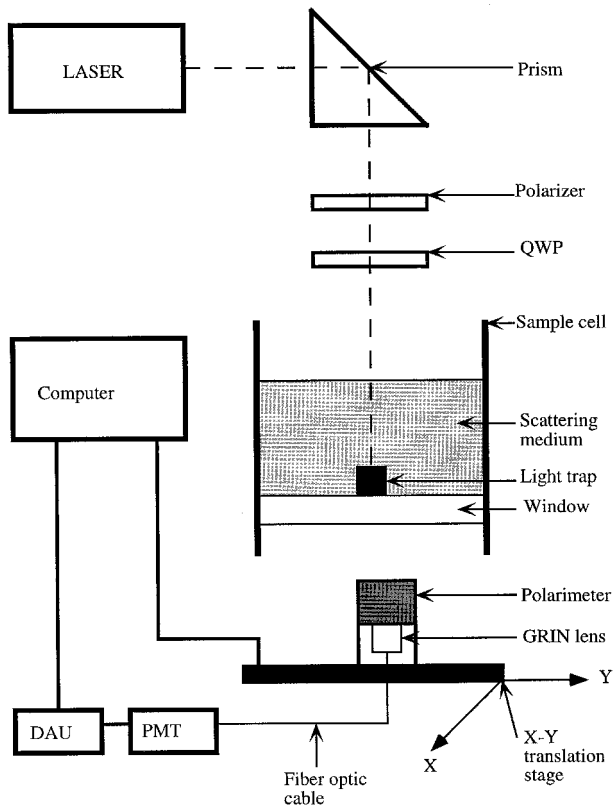

Fig. 4 Schematic of the experimental setup.

of the translation stage is controlled by two stepper motors. Radiation from the polarimeter is collected by a small gradient index lens with a field of view of approximately 3 deg and passed into a 100-μm fiber optic cable. The radiation leaving the fiber optic cable is incident on a photomultipler tube (PMT). The PMT is mounted in a thermoelectrically cooled housing to reduce noise in the output voltage. Current from the PMT is dropped across a high resistance and the resulting voltage is measured by a Hewlett–Packard data acquisition unit (DAU). The DAU and the position of the X–Y translation stage are controlled by a HP-BASIC program from an IBM PC-AT. Note that the entire experimental setup was mounted on vibration isolation pads.

B. Polarimeter

A classical polarimeter arrangement[33–36] used to measure the Stokes vector of an incident light beam is shown in Fig. 5. Other possible methods for measuring the Stokes vector are outlined in Refs. 33, 35, 37, and 38. The arrangement used in this paper consists of a stationary linear polarizer combined with a rotatable linear retarder. The angle of rotation of the retarder with respect to the polarization axis of the linear polarizer is ρ. $\boldsymbol{I}_i$ $(\{I_i, Q_i, U_i, V_i\}^T)$ is the Stokes vector of the incident light beam, and $\boldsymbol{I}_e$ $(\{I_e, Q_e, U_e, V_e\}^T)$ is the Stokes vector of the radiation that leaves the polarimeter and is incident on the detection system. The advantage of using a stationary polarizer is that the optics after the polarizer will always see the same state of polarization, which obviates the need for optics to compensate for possible polarization dependence in the detection optics. Using a technique similar to Ref. 37, the detected intensity is derived to be

$$\frac{2I_e}{t_1 t_2} = I_i + \frac{Q_i}{2}(1 + \cos\delta) - V_i \sin\delta \sin 2\rho + \frac{Q_i}{2}(1 - \cos\delta)\cos 4\rho + \frac{U_i}{2}(1 - \cos\delta)\sin 4\rho \tag{11}$$

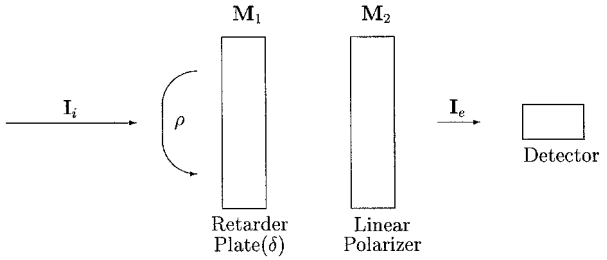

Fig. 5 Schematic of a polarimeter. I_i is the incident Stokes vector, and I_e is the Stokes vector of the radiation leaving the polarimeter.

where t_1 and t_2 are the isotropic transmittances of the retarder and linear polarizer, respectively. The linear polarizer was cut from a polaroid sheet. The retarder used in this experimental study had a retardance (ρ) of 82.9 deg and was rotated to 11 angles between 0 and 180 deg, where the detected voltage was measured. The experimental data were then fit to Eq. (11) to obtain the incident Stokes vector ($\{I_i, Q_i, U_i, V_i\}^T$). Comparison with some known incident polarized sources of radiant energy indicated a possible error of approximately 5% in the data. In our experiment, we focused on relative quantities such as the degree of polarization, and so determination of the transmittances t_1 and t_2 was not required.

IV. Experimental Procedure and Data Reduction

In this section the experimental procedure will be outlined as well as the data reduction methodology.

A. Experimental Procedure

The scatterers used in this study were monodisperse latex spheres. They were obtained as 10% by weight of solids suspended in distilled water. Before use, the suspensions were ultrasonically agitated to ensure that the particles had not coalesced. A sample solution was prepared for each run as indicated by Table 1. This was done by mixing 250 cc (V) of distilled water with a measured amount v of the 10% latex solution with particles of a known diameter D. The amount of 10% latex solution solution required for a given L and χ is given in Table 1. The volumes v shown were calculated with the aid of Eq. (10). Also note that the value of the liquid carrier refractive index (distilled water) was taken to be $n_m = 1.333$, as pointed out in Ref. 35. The sample cell was then cleaned thoroughly and the suspension placed in it. The system was initially aligned so that the laser beam was incident perpendicular to the sample solution. The laser was turned on about 3 h prior to each experimental run, so that the laser output was stable. For each experimental run, the beam power P_{beam} was then measured using a laser power meter.

After the previous preparation, experimental measurements were made. The retarder angle ρ was set to 0 deg, and the voltage measurements from the PMT were taken at 14 data points at radial distances from 0.750–4.000 cm. This was done by scanning the controller of the X–Y translation stages. At each radial location point, 50 voltage samples were taken and averaged to give the voltage magnitudes. The previous procedure was then repeated for 10 more polarimeter retarder angles ρ of 10, 30, 50, 70, 90, 110, 130, 150, 170, and 180 deg. These voltages at each radial location and for each polarimeter retarder angle constituted the raw data for this experiment and were stored in the computer.

B. Data Reduction

In this section the conversion of the raw data to quantities of interest in this study will be dealt with. As mentioned in the previous subsection, the raw data were the voltage obtained at each retarder angle and at each radial location. Based on Eq. (11), data were fit to the following equation:

$$V_e = a_1 + a_2 \cos 2\rho + a_3 \sin 2\rho + a_4 \cos 4\rho + a_5 \sin 4\rho \tag{12}$$

Table 1 Sample solution characteristics for light at 632.8 nm[a]

D, μ	χ	NC_{sca}, cm^{-1}	L 1.0	L 2.0	L 4.0
0.065	0.430	30.806	2.451	4.902	9.804
0.241	1.592	781.64	0.097	0.193	0.386
0.360	2.379	1488.9	0.051	0.102	0.204
0.494	3.264	2205.8	0.034	0.068	0.136

[a]The last three columns contain the volumes v of 10% latex solution (in cc) which are mixed with 250 cc (V) of distilled water to obtain a given optical thickness L.

Note that the coefficients a_1, a_3, a_4, and a_5 are dependent on the Stokes vectors of the incident radiation. The coefficent a_2 was included in the fit to account for additional harmonics in the voltage output. This procedure was necessitated because a Fourier transform of the voltage output showed an additional spike for the cos 2ρ term. This spike was caused by beam wander over the face of the GRIN lens.[38] Within the range of interest in this study, the intensity of the radiation hitting the GRIN lens I_e was found to be linearly proportional to the detected voltage V_e:

$$I_e = KV_e \tag{13}$$

where K is a constant of proportionality for the PMT and can be found experimentally. Thus, based on Eq. (11)

$$Q_i = \frac{2K}{t_1 t_2} \frac{2}{(1 - \cos \delta)} a_4 \tag{14a}$$

$$U_i = \frac{2K}{t_1 t_2} \frac{2}{(1 - \cos \delta)} a_5 \tag{14b}$$

$$V_i = \frac{2K}{t_1 t_2} \frac{1}{\sin \delta} a_3 \tag{14c}$$

$$I_i = \frac{2K}{t_1 t_2} \left(a_1 - \frac{1 + \cos \delta}{1 - \cos \delta} a_4 \right) \tag{14d}$$

As can be seen in Eqs. (14), the experimentally obtained Stokes vectors are all proportional to a constant $2K/t_1t_2$. Thus, ratios of the Stokes vectors, such as the various degrees of polarization, are independent of this constant. Because the goal of this experimental study was primarily to determine the spatial variation in the degrees of polarization, an estimate of K was not required. In the next section of this paper, some plots of intensity I are presented. These plots are essentially the quantity in parentheses in Eq. (14d). Thus, based on Eqs. (3), (14a), (14b), and (14d), the degree of linear polarization is given by

$$P_l = 2 \frac{\sqrt{a_4^2 + a_5^2}}{[a_1(1 - \cos \delta) - a_4(1 + \cos \delta)]} \tag{15}$$

Further, based on Eqs. (4), (14c), and (14d), the degree of circular polarization is given by

$$P_c = \frac{a_3(1 - \cos \delta)}{\sin \delta [a_1(1 - \cos \delta) - a_4(1 + \cos \delta)]} \tag{16}$$

Using the preceding expressions for P_l and P_c, the total degree of polarization P_t can be obtained using Eq. (5).

V. Results

In this section results of this experimental study will be presented. In a later part of this report, comparisons of these data with some Monte Carlo simulations will also be presented. As mentioned earlier, the results to be presented in this

paper are those of a circularly polarized laser beam incident on a plane-parallel scattering suspension. The goal of this paper is to analyze the forward-scattered diffuse radiation. The main parameters used are the degree of linear polarization and the degree of circular polarization. Intensity variations will also be presented; however, as mentioned earlier, the intensities are in arbitrary units. Note that the abscissa in these plots will be either r (optical units) or R (cm). These plots are for the cases outlined in Table 1 (which are for three distinct optical thicknesses and four different size parameters).

A. Intensity

In this section the intensity of the diffusely scattered radiation will be presented. All of the results were normalized by dividing by P_{beam}. In Fig. 6, a plotted quantity proportional to the incident intensity is shown. As is evident from the data, the intensity appears to drop off in a monotonic fashion at higher optical radii. Further, the variation of intensity with respect to particle size is greater at smaller optical thicknesses. The variation in the forward-scattered intensity decreases at larger optical radii for higher optical thicknesses. Note that for a fixed particle size and optical radius, the intensity actually increased with an increase in the optical thickness. This is a result of increased multiple scattering. It would be expected that with for sufficiently large optical thicknesses, the intensity would decrease because of a concurrent increase in the attenuation.

B. Degree of Linear Polarization

In this section the experimentally determined P_l will be presented. Figure 7 illustrates the degree of linear polarization as a function of the optical radius. For all four size parameters

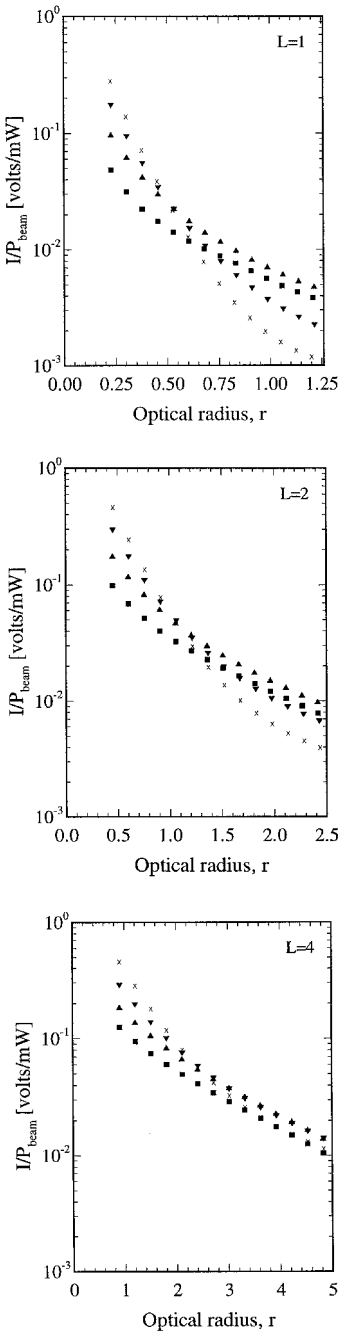

Fig. 6 Variation of intensity with respect to the optical radius for a given optical thickness of the medium (□, x = 0.430; △, x = 1.592; ▽, x = 2.379; ◇, x = 3.264).

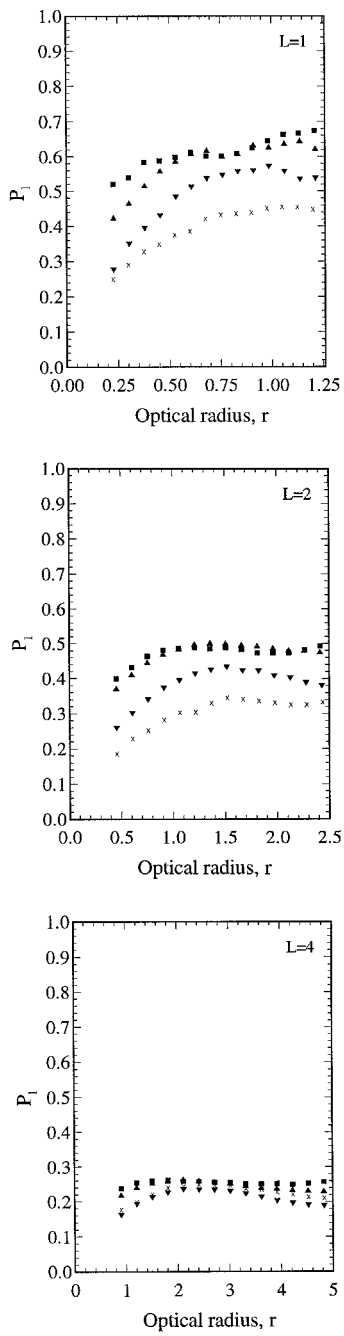

Fig. 7 Variation of the degree of linear polarization with respect to the optical radius for a given optical thickness of the medium (□, x = 0.430; △, x = 1.592; ▽, x = 2.379; ◇, x = 3.264).

considered, an increase in the optical thickness resulted in a decrease in the degree of linear polarization. For all size parameters and at all optical thicknesses considered, the degree of linear polarization initially increased and then stayed relatively constant as the optical radius increased. This is unexpected,[21] because one would expect that at increased optical radii from the laser beam, the increased multiple scattering would depolarize the scattered radiation. As is evident in Fig. 7, this is clearly not the case.

In Fig. 7 each graph shows the effect of the scatter size parameter on the degree of linear polarization for a fixed optical thickness of the scattering medium. Clearly, for increased optical thicknesses, the differences between the various size parameters decrease at larger optical radii. The trend of the data suggests that at larger optical radii, the larger size parameters cause the diffuse radiation to be less polarized compared to the smaller size parameter scatterers. The data at $L = 4$ (Fig. 7) shows the degree of linear polarization to be almost indistinguishable for all four size parameters at such a high optical thickness. In Fig. 7, the differences in the degree of linear polarization between the particles for size parameters of 0.430 and 1.592 were negliglible at all three optical thicknesses illustrated. This can be explained by the fact that the elements of the scattering matrices for particles with these size parameters are very similar to each other, as shown in Fig. 3.

In Fig. 8 the abscissa is the geometric radius R (cm), increased from the laser beam center. Also, in Fig. 8, it can be seen that as the number density of scatterers is increased, the degree of linear polarization decreases. It should be noted that doubling of the optical thickness was achieved by doubling the number density of scatterers. Over the radial domain of measurement, the degree of linear polarization increases to a relatively constant value for all cases considered in this study.

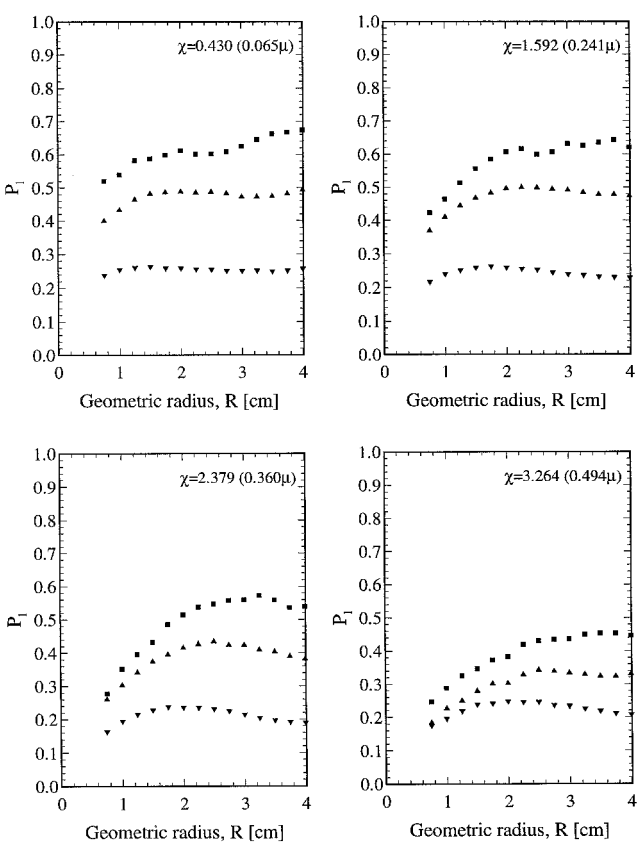

Fig. 8 Variation of the degree of linear polarization with respect to the geometric radius for a given size parameter (□, $L = 1$; △, $L = 2$; ▽, $L = 4$).

C. Degree of Circular Polarization

In this section P_c will be examined. Figure 9 shows the degree of circular polarization plotted with respect to the optical radius. The degree of circular polarization shows significant variations with respect to size parameter and optical thickness of the medium. For all size parameters of interest, it can be observed that the degree of circular polarization is actually higher for larger optical thicknesses of the medium. Thus, for a fixed optical radius from the laser beam, the medium with a higher optical thickness exhibits a higher degree of polarization. Further, it can be seen that irrespective of optical thickness, the degree of circular polarization for a given size parameter approaches a unique value for all optical thicknesses considered at small optical radii from the beam. This can be seen most clearly for size parameters of 2.379 and 3.264.

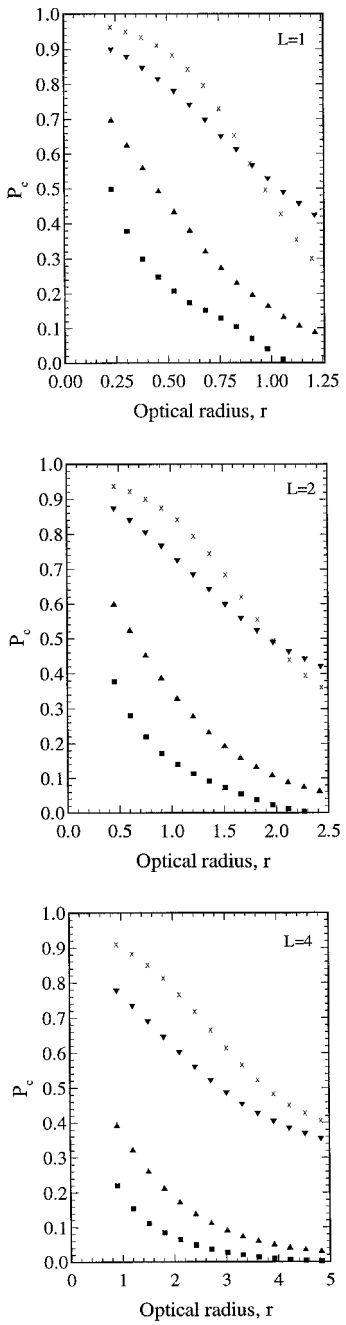

Fig. 9 Variation of the degree of circular polarization with respect to the optical radius for a given optical thickness of the medium (□, $x = 0.430$; △, $x = 1.592$; ▽, $x = 2.379$; ◇, $x = 3.264$).

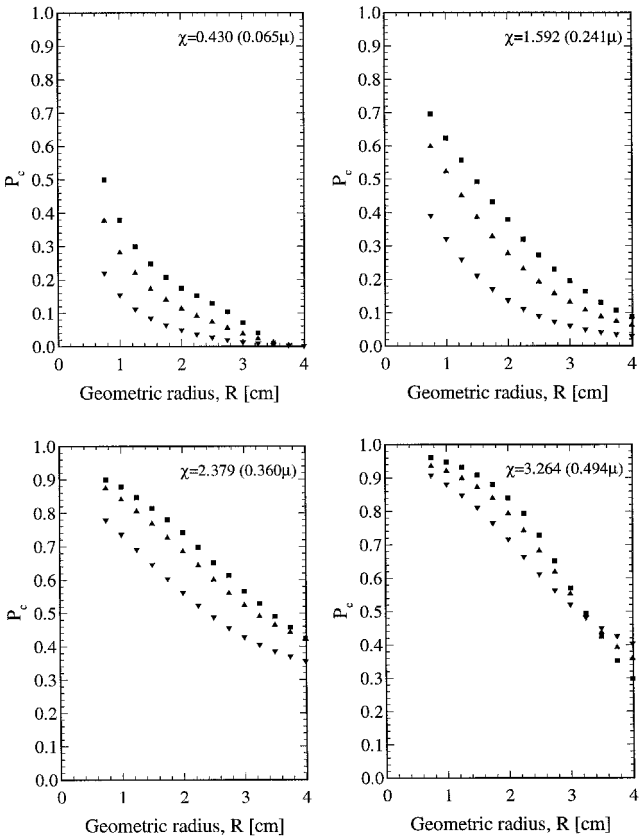

Fig. 10 Variation of the degree of circular polarization with respect to the geometric radius for a given size parameter (□, L = 1; △, L = 2; ▽, L = 4).

In Fig. 9 it is seen that for all optical thicknesses considered, the degree of circular polarization in the case of a size parameter of 0.430 approaches zero. Further, at larger optical radii, the degree of circular polarization actually seems to level off at a nonzero value for larger size parameters. The trends of these graphs suggest that at large optical radii from the laser beam, larger particles will result in the diffuse radiation having a greater degree of circularly polarization. Unlike the degree of linear polarization, the degree of circular polarization showed a greater sensitivity to smaller-size parameters as compared to the larger-size parameters.

In Fig. 10, the abscissa is the geometric radius R (cm) from the laser beam center. In these plots, it can be clearly seen that as the number density of scatterers is increased, the degree of circular polarization decreases. Again, it should be noted that doubling of the optical thickness was achieved by doubling the number density of scatterers.

D. Degree of Polarization

The total degree of polarization P_t exhibits trends that are a mixture of the trends observed in the previous two sections and are as shown in Fig. 11. In fact, the behavior varies considerably. For smaller size parameters, the degree of polarization has a similar trend to the degree of linear polarization with respect to the optical radius and the optical thickness of the medium, respectively. At larger size parameters, the behavior more closely echos the behavior of the degree of circular polarization. The main observation for Fig. 11 was that the diffuse radiation was polarized at quite substantial optical radii from the laser beam. Further, at larger optical thicknesses, particles with a larger-size parameter produced a greater degree of polarization.

E. Comparison with Monte Carlo Simulations

In the following text some of the experimental data involving the degree of polarization of the diffuse radiation will be

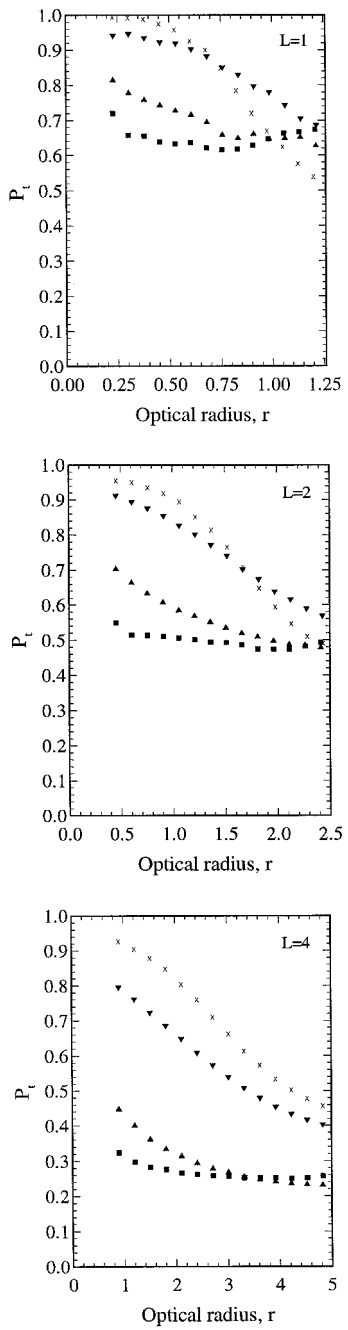

Fig. 11 Variation of the total degree of polarization with respect to the optical radius for a given optical thickness (L) of the medium (□, x = 0.430; △, x = 1.592; ▽, x = 2.379; 3 , x = 3.264).

compared with numerical data generated using a backward Monte Carlo code developed by the authors.[18] The elements of the scattering matrix [see Eq. (6)] used in the backward Monte Carlo code for the evaluation of the forward-scattered diffuse radiation had values as shown in Fig. 3. However, the computer code did not include the Fresnel reflection effects at the water–window and water–glass interfaces. This would definitely affect the results because Fresnel reflection can have a strong polarizing effect.[34] Further, the data generated for this paper assumed that the energy of the laser was concentrated at one point. This is actually not the case, but because the numerical data were taken at a significant number of beam diameters from the laser, this seemed an acceptable assumption. The present comparisons were made to see if the Monte Carlo code captured the trends in the degree of polarization with respect to particle size and optical thickness of the me-

dium. One other point of importance is that the numerical data were evaluated out to an optical radius of 3.0, and 400,000 photons were used to evaluate the Stokes vector at each location. Further, the ω of the scatterers was taken to be one in this study.

In Fig. 12, comparison is made between the experimental and numerical data for the particles of size parameter of 0.430. At all optical depths shown in Fig. 12, P_c matched well with the experimental results. For both cases, the degree of circular polarization decayed to a value close to zero. Comparison of the degree of linear polarization showed greater differences. The differences between the experimental and Monte Carlo data decreased with an increase in the optical thickness of the medium. At optical radii greater than 1.0, the Monte Carlo evaluated degree of linear polarization consistently underpredicted the experimental data. One possible reason for this could be the fact that a Fresnel interface has a reflection matrix similar in form to a linear polarizer.[34] The curves shown in Fig. 13 are similar to those just discussed, except that they are for a size parameter of 2.379. In Fig. 13, it can be seen that the trends in both the degree of circular polarization and the degree of linear polarization are captured by the Monte Carlo procedure. However, the degree of linear polarization is consistently underpredicted by this procedure. Another interesting feature is that at small optical radii, the Monte Carlo data and the experimental data asymptotically approach each other for all three optical thicknesses of the medium. In both Figs. 12 and 13, it can be seen that the degree of linear polarization remains relatively constant to quite large optical radii.

F. Mean Number of Scattering Events

In the following discussion, a quantity called the mean number of scattering events Γ will be discussed. It is a measure of

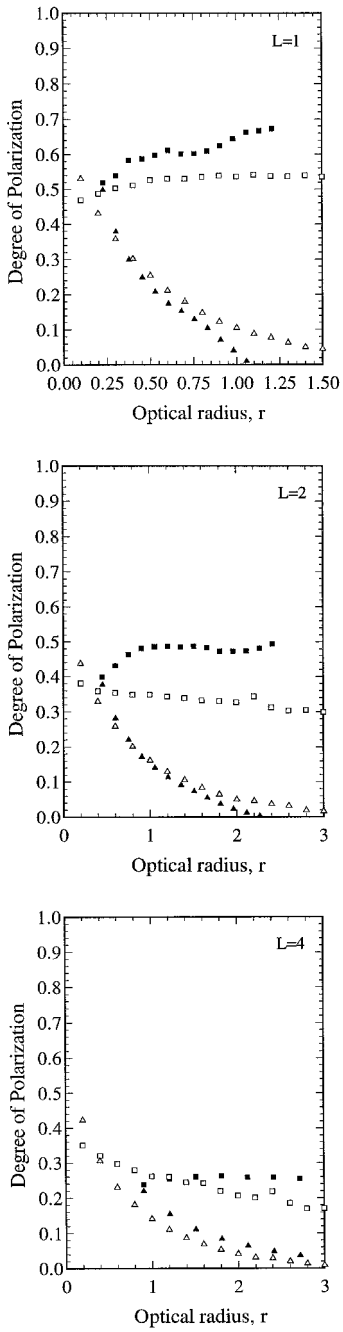

Fig. 12 Comparison of P_l and P_c with backward Monte Carlo simulations for x = 0.430 [□, P_l (experiment); △, P_c (experiment); □, P_l (Monte Carlo); △, P_c (Monte Carlo)].

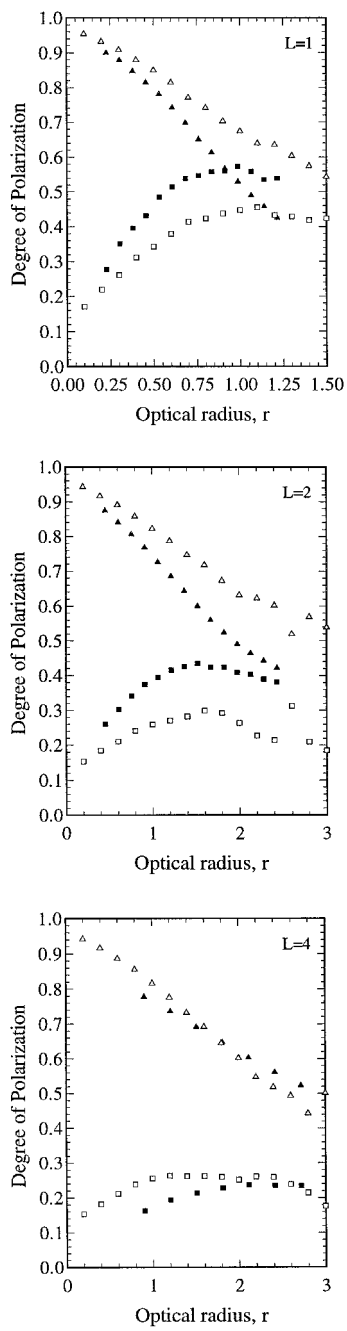

Fig. 13 Comparison of P_l and P_c with backward Monte Carlo simulations for x = 2.379 [□, P_l (experiment); △, P_c (experiment); □, P_l (Monte Carlo); △, P_c (Monte Carlo)].

the average number of scattering events a photon would undergo to reach a particular location.[18] In Fig. 14, the mean number of scattering events is plotted for the Monte Carlo data outlined in the previous paragraph. The plots of Γ are only for the data obtained excluding Fresnel effects at the interface between the liquid and the surrounding medium (water–air and water–glass interfaces). The mean number of scattering events cannot be evaluated experimentally. The purpose of plotting this data is to illustrate that the diffuse radiation is polarized even after a large number of scattering events. Although the experimental data includes the Fresnel effects, the purpose of this section is to illustrate that for large optical radii from the laser beam, the diffuse radiation is polarized despite the large number of scattering events a photon must undergo. This seems at variance to the theoretical work of Bicout and Brosseau.[21] As shown in Fig. 14, even at an optical radius of 3.0, the average number of scattering events exceeds 12 for the particles of size parameter 0.430, and it exceeds 7 for particles of size parameter 2.379. For some of the cases discussed, experimental measurements were taken up to an optical radius of 5.0. In such cases, the mean number of scattering events would be still higher. Despite this, the diffuse radiation is polarized even at these large optical radii. Clearly, the diffuse radiation is polarized (see Figs. 12 and 13) at the optical radii and optical thicknesses illustrated in Fig. 14. This is interesting because, as mentioned in a previous section, one would expect that a large number of scattering events would depolarize the radiation. In fact, only the degree of circular polarization for small-size parameters behaves in this way (see Fig. 12). It should be noted here that the data for $L = 1$ shown plotted in Fig. 14 was only to an optical radius of 1.5. This was because our experimental data for this optical thickness were limited to this radius.

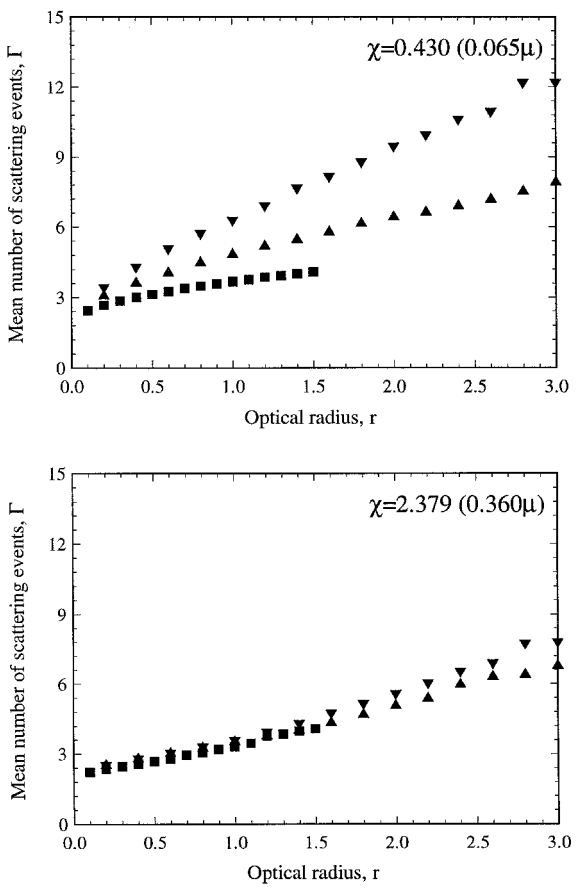

Fig. 14 Mean number of scattering events as a function of the optical radius from the incident light beam (□, $L = 1$; △, $L = 2$; ▽, $L = 4$).

VI. Conclusions

In this experimental study, the forward-scattered diffuse radiation was examined for the case of a right circularly polarized laser beam incident on a plane-parallel scattering medium. Results of this study were compared to a Monte Carlo simulation of the same situation excluding Fresnel interface effects. The numerical data exhibited similar trends to the experimental work.

The results of this study were very interesting. The data suggests that the diffuse radiation produced by a finite multiple scattering media when exposed to a circularly polarized laser beam is significantly polarized, even at large optical radii from the beam. Monte Carlo simulations indicated a similar trend. Further, an estimate of the average number of scattering events a photon would undergo to reach reasonably large optical radii suggests that the diffuse radiation there is highly multiply scattered because of the large average number of scattering events to reach that location. This is unexpected because one would expect that the large number of scattering events required to reach a large optical radius would depolarize the diffuse radiation. This is clearly not the case.

Further research is required into the effect of the refractive index of the medium (water in this study) on the degree of polarization of the emerging diffuse light field for the problem studied in this paper. The refractive index manifests itself via the reflection at the air–water and water–glass interfaces. It is well known that reflection at the interface between two media can polarize the incident radiation.

Acknowledgments

The authors wish to acknowledge the partial support of the National Science Foundation through Grant CTS-9633615. The authors also wish to thank the reviewers of this paper for their careful reading of the material and their numerous invaluable suggestions.

References

[1]Kienle, A., Lilge, L., Patterson, M. S., Hibst, R., Steiner, R., and Wilson, B. C., "Spatially Resolved Absolute Diffuse Reflectance Measurements for Noninvasive Determination of the Optical Scattering and Absorbtion Coefficients of Biological Tissue," *Applied Optics*, Vol. 35, No. 13, 1996, pp. 2304–2314.

[2]Wang, L., and Jacques, S. L., "Hybrid Model of Monte Carlo Simulation and Diffusion Theory for Light Reflectance by Turbid Media," *Journal of the Optical Society of America*, Vol. 10, No. 8, 1993, pp. 1746–1752.

[3]Groenhuis, R. A. J., Ferwada, H. A., and Ten Bosch, J. J., "Scattering and Absorption of Turbid Materials Determined from Reflection Measurements. 1: Theory," *Applied Optics*, Vol. 22, No. 16, 1983, pp. 2456–2462.

[4]Wilson, B. C., and Adams, G., "A Monte Carlo Model for the Absorbtion and Flux Distributions of Light in Tissue," *Medical Physics*, Vol. 10, No. 6, 1983, pp. 824–830.

[5]Bissonnette, L. R., Bruscaglioni, P., Ismaelli, A., Zaccanti, G., Cohen, A., Benyahu, Y., Kleiman, M., Egert, S., Flesia, C., Schwendimann, P., Starkov, A. V., Noormohammadian, M., Oppel, U. G., Winkler, D. M., Zege, E. P., Katsev, I. L., and Polonsky, I. N., "LIDAR Multiple Scattering from Clouds," *Applied Physics*, Vol. B, No. 60, 1995, pp. 355–362.

[6]Yamazaki, H., Tojo, K., and Miyanami, K., "Measurement of Local Solids Concentration in a Suspension by an Optical Method," *Powder Technology*, Vol. 70, No. 1, 1992, pp. 93–96.

[7]Carswell, A. I., and Pal, S. R., "Polarization Anisotropy in Lidar Multiple Scattering from Atmospheric Clouds," *Applied Optics*, Vol. 24, No. 21, 1985, pp. 3464–3471.

[8]Look, D. C., Jr., "Anisotropy of the Lateral Scattering of Linearly Polarized Light," *Optical Engineering*, Vol. 28, No. 2, 1989, pp. 160–164.

[9]Look, D. C., Jr., and Chen, Y. R., "Study of Polarization of Laser Radiation Scattered 90°," *Journal of Thermophysics and Heat Transfer*, Vol. 7, No. 4, 1993, pp. 631–636.

[10]Look, D. C., Jr., and Chen, Y. R., "Examination of Scattering at 90° from a Cylindrical Volume Illuminated by Polarized Light," *Applied Optics*, Vol. 34, No. 1, 1995, pp. 144–151.

[11]Dogariu, M., and Asakura, T., ''Polarization-Dependent Backscattering Patterns from Weakly Scattering Media,'' *Journal of Optics (Paris)*, Vol. 24, No. 6, 1993, pp. 271–278.

[12]Dogariu, M., and Asakura, T., ''Reflectance Properties of Finite-Size Turbid Media,'' *Waves in Random Media*, Vol. 4, 1994, pp. 429–439.

[13]Mueller, D. W., Jr., and Crosbie, A. L., ''Three-Dimensional Radiative Transfer with Polarization in a Multiple Scattering Medium Exposed to Spatially Varying Radiation,'' *Journal of Quantitative Spectroscopy and Radiative Transfer*, Vol. 57, No. 1, 1997, pp. 81–105.

[14]Mueller, D. W., Jr., and Crosbie, A. L., ''Three-Dimensional Radiative Transfer: Radiation Emergent from a Multiple Scattering Medium Exposed to a Polarized Laser Beam, *Journal of Quantitative Spectroscopy and Radiative Transfer* (submitted for publication).

[15]Collins, D. G., Blättner, W. G., Wells, M. B., and Horak, H. G., ''Backward Monte Carlo Calculations of the Polarization Characteristics of the Radiation Emerging from Spherical-Shell Atmospheres,'' *Applied Optics*, Vol. 11, No. 11, 1972, pp. 2684–2696.

[16]Marchuk, G. I., Mikhailov, G. A., Nazaraliev, M. A., Darbinjan, R. A., Kargin, B. A., and Elepov, B. S., *The Monte Carlo Methods in Atmospheric Optics*, Springer–Verlag, Berlin, 1980.

[17]Ambirajan, A., and Look, D. C., Jr., ''A Backward Monte Carlo Estimator for the Multiple Scattering of a Narrow Light Beam,'' *Journal of Quantitative Spectroscopy and Radiative Transfer*, Vol. 56, No. 3, 1996, pp. 317–336.

[18]Ambirajan, A., and Look, D. C., Jr., ''A Backward Monte Carlo Study of the Multiple Scattering of a Polarized Laser Beam,'' *Journal of Quantitative Spectroscopy and Radiative Transfer* (to be published).

[19]Look, D. C., Jr., and Chen, Y. R., ''Comparison of Linearly and Circularly Polarized Incident Light Scattered 90°,'' AIAA Paper 94-2093, June 1994.

[20]Look, D. C., Jr., ''Comparisons in Back-Scatter and Radial-Scatter of Incident Linearly and Circularly Polarized Light,'' *Polarization Considerations for Optical Systems II*, Vol. 1166, SPIE—the International Society for Optical Engineers, 1989, pp. 518–532.

[21]Bicout, D., and Brosseau, C., ''Multiply Scattered Waves Through a Spatially Random Medium: Entropy Production and Depolarization,'' *Journal of Physics I (France)*, Vol. 2, 1992, pp. 2047–2063.

[22]Bicout, D., Brosseau, C., Martinez, J. W., and Schmitt, J. M., ''Depolarization of Multiply Scattered Waves by Spherical Diffusers: Influence of Size Parameter,'' *Physical Review E*, Vol. 49, No. 2, 1994, pp. 1767–1770.

[23]Vreeker, R., Van Albada, M. P., and Lagendijk, A., ''Depolarization of Femtosecond Laser Pulses in Disordered Media,'' *Optics Communications*, Vol. 70, No. 5, 1989, pp. 365–368.

[24]MacKintosh, F. C., Zhu, J. X., Pine, D. J., and Weitz, D. A., ''Polarization Memory of Multiply Scattered Light,'' *Physical Review B: Solid State*, Vol. 40, No. 13, 1989, pp. 9342–9345.

[25]Hovenier, J. W., and Van der Mee, C. V. M., ''Fundamental Relationships Relevant to the Transfer of Polarized Light in a Scattering Atmosphere,'' *Astronomy and Astrophysics*, Vol. 128, 1983, pp. 1–16.

[26]Voss, K. J., and Fry, E. S., ''Measurement of the Mueller Matrix for Ocean Water,'' *Applied Optics*, Vol. 23, No. 23, 1984, pp. 4427–4439.

[27]Bohren, C. F., and Huffman, D. R., *Absorbtion and Scattering of Light by Small Particles*, Wiley, New York, 1983.

[28]H. C. Van de Hulst, *Light Scattering by Small Particles*, Dover, New York, 1981.

[29]Dave, J. V., ''Coefficients of the Legendre and Fourier Series for the Scattering Functions of Spherical Particles,'' *Applied Optics*, Vol. 9, No. 8, 1970, pp. 1888–1896.

[30]Wiscombe, W. J., ''Improved Mie Scattering Algorithms,'' *Applied Optics*, Vol. 19, No. 9, 1980, pp. 1505–1509.

[31]Mischenko, M. I., Travis, L. D., and Mackowski, D. W., ''T-Matrix Computations of Light Scattering by Nonspherical Particles,'' *Journal of Quantitative Spectroscopy and Radiative Transfer*, Vol. 55, No. 5, 1980, pp. 535–575.

[32]Nelson, H. F., Look, D. C., Jr., and Crosbie, A. L., ''Two-Dimensional Radiative Back-Scattering from Optically Thick Media,'' *Journal of Heat Transfer*, Vol. 108, 1992, pp. 619–625.

[33]Look, D. C., Jr., ''Novel Stokesmeter,'' *Journal of Thermophysics and Heat Transfer*, Vol. 10, No. 3, 1996, pp. 536–539.

[34]Van de Hulst, H. C., *Multiple Light Scattering*, Academic, New York, 1980.

[35]Collett, E., *Polarized Light: Fundamentals and Applications*, Marcel Dekker, New York, 1993.

[36]Kliger, D. S., Lewis, J. W., and Randall, C. E., *Polarized Light in Optics and Spectroscopy*, Academic, Boston, 1990.

[37]Ambirajan, A., and Look, D. C., Jr., ''Optimum Angles for a Polarimeter: Part I,'' *Optical Engineering*, Vol. 34, No. 6, 1995, pp. 1651–1655.

[38]Goldstein, D. H., ''Mueller Matrix Dual-Rotating Retarder Polarimeter,'' *Applied Optics*, Vol. 31, No. 31, 1992, pp. 6676–6683.